8608 J. Med. Chem. 2010, 53, 8608–8618
DOI: 10.1021/jm100801e

Journal of Medicinal Chemistry Article

Benzimidazol-2-ylidene Gold(I) Complexes Are Thioredoxin Reductase Inhibitors with Multiple Antitumor Properties

Riccardo Rubbiani,[†] Igor Kitanovic,[‡] Hamed Alborzinia,[‡] Suzan Can,[‡] Ana Kitanovic,[‡] Liliane A. Onambele,[§] Maria Stefanopoulou,[∥] Yvonne Geldmacher,[∥] William S. Sheldrick,[∥] Gerhard Wolber,[⊥] Aram Prokop,[§] Stefan Wölfl,[‡] and Ingo Ott*[,†]

[†]*Institute of Pharmaceutical Chemistry, Technische Universität Braunschweig, Beethovenstrasse 55, 38106 Braunschweig, Germany,* [‡]*Institut für Pharmazie und Molekulare Biotechnologie, Ruprecht-Karls-Universität Heidelberg, Im Neuenheimer Feld 364, 69120 Heidelberg, Germany,* [§]*Department of Paedriatric Oncology, Childrens Hospital Cologne, Amsterdamer Strasse 59, 50735 Cologne, Germany,* [∥]*Lehrstuhl für Analytische Chemie, Ruhr-Universität Bochum, 44780 Bochum, Germany, and* [⊥]*Institute of Pharmacy, Freie Universität Berlin, Königin-Luise-Strasse 2 + 4, 14195 Berlin, Germany*

Received June 29, 2010

Gold(I) complexes such as auranofin have been used for decades to treat symptoms of rheumatoid arthritis and have also demonstrated a considerable potential as new anticancer drugs. The enzyme thioredoxin reductase (TrxR) is considered as the most relevant molecular target for these species. The here investigated gold(I) complexes with benzimidazole derived *N*-heterocyclic carbene (NHC) ligands **1a**−**4a** represent a promising class of gold coordination compounds with a good stability against the thiol glutathione. TrxR was selectively inhibited by **1a**−**4a** in comparison to the closely related enzyme glutathione reductase, and all complexes triggered significant antiproliferative effects in cultured tumor cells. More detailed studies on a selected complex (**2a**) revealed a distinct pharmacodynamic profile including the high increase of reactive oxygen species formation, apoptosis induction, strong effects on cellular metabolism (related to cell surface properties, respiration, and glycolysis), inhibition of mitochondrial respiration and activity against resistant cell lines.

Introduction

Cisplatin and other platinum species belong to the blockbusters of anticancer drugs sold worldwide. However, remaining problems such as severe side effects and resistance phenomena trigger an increasing demand for novel innovative drugs with a mode of action differing from that of the platinum generation of cancer chemotherapeutics.[1−3] In recent years especially, gold complexes have attracted major attention due to their enzyme inhibiting acitivities related to cancer development and progression (e.g., interaction with cathepsins, tyrosine phosphatases, or cyclooxygenases). The antirheumatic gold(I) phosphine drug auranofin emerged as the lead compound also for the class of antiproliferatively active gold species, and in the recent years, an increasing number of bioactive complexes (e.g., phosphine derivatives, gold carbene complexes, or several gold(III) agents) have shown promising biological activity (see Figure 1 for some relevant examples).[4−12]

On the basis of the structural diversity of the reported complexes and the huge amount of so far available biological data, a common mode of action for gold complexes is unlikely to exist. However, the enzyme thioredoxin reductase (TrxR[a]) is nowadays considered as the most relevant target for bioactive gold coordination compounds.[5−7] Human TrxR is an enzyme belonging to the antioxidant cellular network and involved in many aspects of tumor pathophysiology (e.g., proliferation, apoptosis, metastasis). It is an ubiquitary NADPH-dependent flavoprotein with a cysteine-cysteine bridge at the N-terminal end and a selenocysteine-cysteine bridge at the C-terminal end (also termed the interface domain of the protein), from which it differs from the otherwise closely related enzyme glutathione reductase (GR).[13,14] Gold complexes derived from the lead compound auranofin have demonstrated a considerable selectivity for the inhibition of TrxR over GR or other structurally similar enzymes.[8,15,16] This selectivity is commonly attributed to the higher affinity of gold for selenium (as present

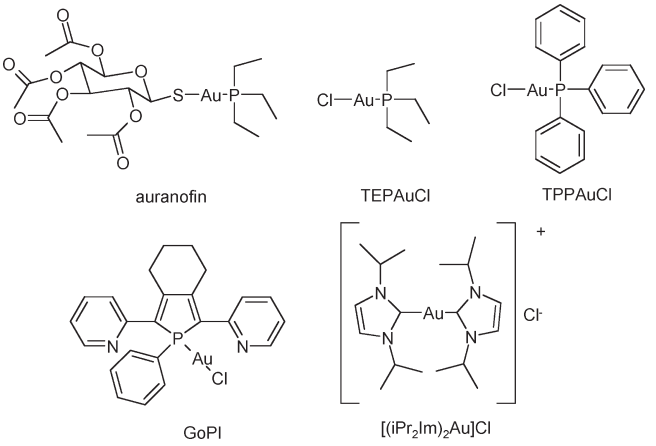

Figure 1. Bioactive gold(I) species.

*To whom correspondence should be addressed. Phone: +49 531 3912743. Fax: +495313918456. E-mail: ingo.ott@tu-bs.de.

[a] Abbreviations: GR, glutathione reductase; LDH, lactate dehydrogenase; NHC, *N*-heterocyclic carbene; TNB, 2-nitro-5-thiobenzoic acid; ROS, reactive oxygen species; DTNB, 5,5′-dithiobis-(2-nitrobenzoic acid); TrxR, thioredoxin reductase.

 Published on Web 11/17/2010

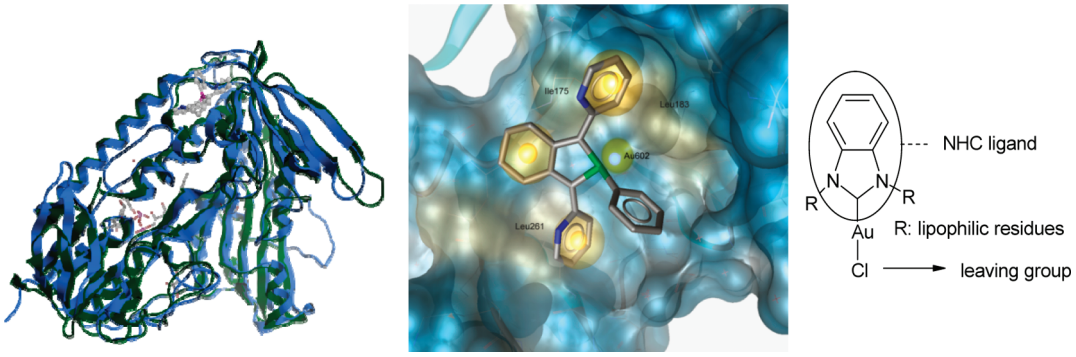

Figure 2. Left: overlay of TrxR (blue) and GR (green). Middle: organic residue of GOPI in GR. Hydrophobic contacts are indicated as yellow spheres, the binding pocket surface is color-coded by hydrophobicity (yellow = hydrophobic, blue = hydrophilic). Right: structural features of the novel target compounds.

in TrxR but not in GR) compared to sulfur and has also been experimentally confirmed by using mutant forms of TrxR as well as by advanced mass spectrometry studies on the C-terminal motif of TrxR.[17,18]

However, auranofin is strongly metabolized and much evidence exists that it represents a prodrug for several bioactive metabolites.[7,19−21] For example, in serum, a conjugate with albumin is readily formed under replacement of the thiolate ligand.[19] So far this instability has prevented a more rational development of novel gold(I) drugs, and it is thus not surprising that the number of available structure−activity relationship studies on auranofin derivatives is rather limited.[4,5,22,23]

Interestingly, in recent years, many highly promising results with novel gold(I) species have been reported, shedding also more light on the issue of drug design.[11,16,17,23−25] For example, for the gold phosphol complex [1-phenyl-2,5-di(2-pyridyl)-phosphole]AuCl (GoPI), which showed EC_{50} values in the low nanomolar range against both TrxR and GR, a crystal structure with GR was published. This provided an experimental proof for the covalent binding of gold to relevant cysteine residues in GR and thereby opened also some options for a more rational design of bioactive gold species.[17,26] Additionally, gold(I) NHC complexes developed by the group of Berners-Price have shown exciting biological properties including the inhibition of TrxR, selectivity for tumorous tissues over normal tissue, apoptosis induction, or preferential binding to selenols over thiols.[25,27−29] NHCs are strong σ-donors stabilized by π-backbonding, which can coordinate with metals to complexes of comparable stability with gold(I) phosphines.[30,31] Thus, NHC gold compounds may also represent a type of bioorganometallics exhibiting an enhanced stability under biologically relevant conditions.[32] The general potential of NHC ligands for the use in drug development is also reflected by an increasing number of studies reporting formidable pharmacological properties for complexes with various metals (including, e.g., silver, platinum) going back to first reports on antimicrobal derivatives.[32−38]

Motivated by the great potential of NHC complexes in drug design and by our recent results with gold(I) species[11,23,24] we developed and studied a series of novel gold(I) NHC complexes. The target compounds are based on a benzimidazol-2-ylidene core and were designed based on available crystal structure data of the gold phosphole GoPI in the active site of GR (see below). The synthesis, stability (against inactivation by glutathione), and the intensive biological investigation are reported here and demonstrate a huge potential of this type of bioorganometallics in medicinal chemistry.

Structural Considerations and Design Strategy of the Target Compounds

For the rational design of new bioactive gold(I) NHC coordination compounds, we used the recently published crystal structure of human GR containing the gold phosphole inhibitor GoPI as a starting point.[17] An initial overlay of human TrxR with human GR (see Figure 2, left) had confirmed the close structural analogy of both protein structures, indicating that the observed binding sites of GoPI in GR could also be used to design potent inhibitors of TrxR. Selectivity for TrxR over GR should finally be achieved due to the higher affinity of the gold central atom to the selenocysteine residue in TrxR compared to the cysteine residue in GR.

GR incubated with GoPI showed two mechanisms taking place: a cross-linking of two cysteines in the active site by a gold atom, which was set free upon complete ligand dissociation of GoPI and the covalent binding of a gold phosphole moiety to the surface exposed Cys-284 under loss of a chloride ligand (see Figure 2 middle).[17] The existence of such structural data opens some options for the structure based design of related potential inhibitors and the development of novel compounds might in turn also provide information on the relevance of the Cys-284 binding site.

Evaluation of the structural features of the gold phosphole attached to Cys-284 indicated that the two pyridine rings and the cyclohexane ring annelated to the phosphol ring were involved in hydrophobic interactions (mainly with Leu-183, Leu-261, and Ileu-175, see Figure 2 middle), whereas the phenyl ring was located outside the binding site. Relevant polar interactions or hydrogen bonding to nearby residues of the GR protein backbone could not be identified. Taking this information into account, we designed a short series of gold(I) NHC species which exhibit the following features: a central benzimidazol-2-ylidene carbene core, substituents with varying lipophilicity and surface volume for an improved interaction with the binding site, and a chloride leaving group enabling the necessary covalent binding (see Figure 2 right).

Synthesis

The target compounds were prepared according to a convenient established procedure starting from benzimidazole (see Scheme 1).[27,39−41] Alkylation of the aromatic nitrogens was achieved by refluxing the educt with an excess of the respective alkyl halogenide in the presence of a mild base in acetonitrile. The benzimidazol-2-ylidene gold complexes were obtained by treating the benzimidazolium salts with Ag_2O

(leading to the formation of an intermediate silver complex) followed by a ligand exchange reaction with chlorodimethylsulfide gold(I). The target compounds were finally purified by filtration over Celite and characterized by ^{1}H NMR, mass spectrometry, and elemental analysis. A characteristic feature confirming the complex formation was the disappearing of the carbene proton signal in ^{1}H NMR spectra upon coordination. ^{13}C NMR spectra were exemplarily taken for **2** and **2a** and again confirmed complex formation as the signal of the carbene carbon was shifted from 141 ppm in **2** to 177 ppm in **2a**.

Reaction with Glutathione

For inactivation of the anticancer drug cisplatin and many other metal based drugs, thiols such as the tripeptide glutathione play an important role. Similarly, the gold(I) phosphine lead compound auranofin is biologically processed and metabolized in thiol ligand exchange processes.[7,19,20] As metal NHC complexes supposedly represent biologically stable coordination compounds, it was of interest to study their interaction with glutathione under physiological conditions in comparison to relevant gold(I) phosphine complexes. Initially, the stability of gold(I) NHC complexes in buffer solution at 37 °C was confirmed exemplarily for **2a** (see Supporting Information, Figure S1).

Scheme 1. Synthesis Procedure for **1a**−**4a**[a]

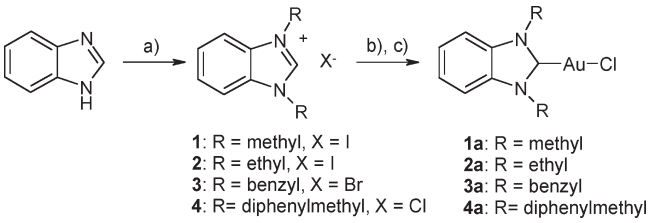

[a] (a) Alkylhalide, K_2CO_3, CH_3CN, reflux, 6 h; (b) Ag_2O in CH_2Cl_2, 6 h; (c) chloro(dimethylsulfide)gold(I), 4 h.

For the subsequent experiments on possible inactivation by glutathione, we used the 5,5′-dithiobis-(2-nitrobenzoic acid) (DTNB, also known as the Ellmans reagent), which can be used to quantify the thiol content of biological samples based on a rapid and stochiometric reaction but which also allows to monitor the activity of NADPH metabolizing enzymes such as TrxR.[15,42−44] In contrast to enzymatic reduction assays where one equivalent of DTNB is reduced under formation of two equivalents of of 2-nitro-5-thiobenzoic acid (TNB, Figure 3a) DTNB reacts with a thiol to a mixed disulfide and one equivalent of TNB (see Figure 3b), which can finally be measured photometrically. The formation of gold complexes at the cysteine thiol of reduced glutathione (or a metal mediated oxidation of the tripeptide) would lower the available amount of free thiol able to react with DTNB. This assay thus provides an efficient tool to screen the stability of gold complexes against inactivation by glutathione.

For the experiments, we incubated an excess of the respective gold complex with reduced glutathione at 37 °C for 20 and 60 min. Chloro(dimethylsulfide)gold(I) (Me_2SAuCl) was used as a positive control and as expected led to an almost complete reduction of TNB product formation under the chosen conditions (see Figure 4).

Quite astonishingly, the gold(I) NHC species **1a**−**4a** did not influence the reaction significantly and can thus be considered as sufficiently stable against thiols under biologically relevant conditions, a property highly desirable in the drug development of novel metal coordination compounds. Only **1a** showed a minor inhibition of approximately 10% after 60 min. This might be attributed to the lower steric hindrance of an attack at the gold center by the less bulky methyl side chains. In fact, ligand replacement processes upon reaction with cysteine over

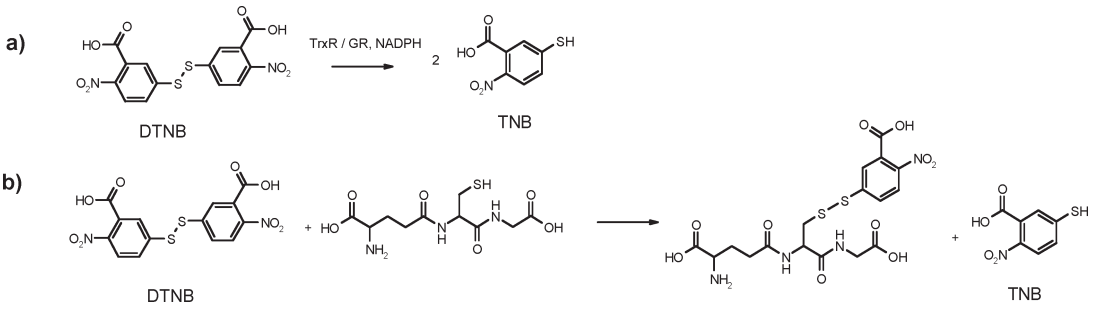

Figure 3. Possible reactions taking place with the Ellmans reagent: (a) reduction by NADPH metabolizing enzymes; (b) disulfide bond exchange with thiols (here reduced glutathione).

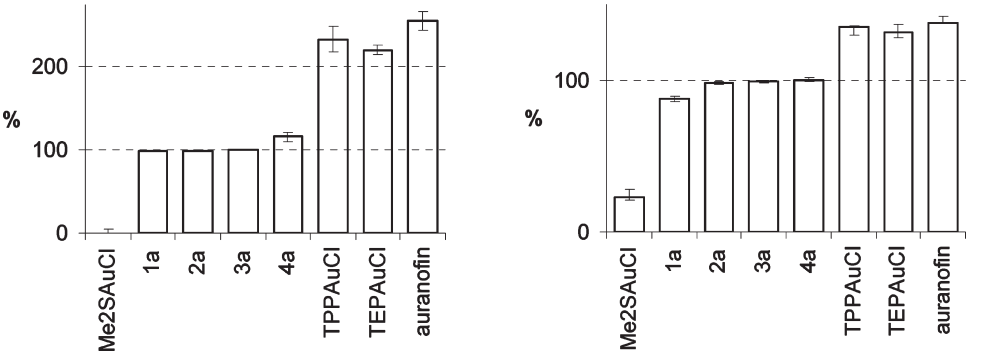

Figure 4. Interaction of gold(I) complexes with glutathione and DTNB; left, 20 min exposure; right, 60 min exposure.

an extended period of time have been reported for gold(I) NHC derivatives.[25]

Unexpectedly, gold(I) phosphine complexes led to a strong increase in TNB release during the reaction, which was most marked after the shorter exposure period (20 min). Due to stochiometric reasons, an exceeding of 100% is not possible (see Figure 3b) and therefore the occurrence of an additional breaking/reduction of the DTNB disulfide bond had to be taken into account. For auranofin, it had been reported that after an initial formation of an albumin-auranofin adduct, in which the thiocarbohydrate was replaced by a cysteine of albumin, the phosphine neutral ligand dissociated off the gold atom and was oxidized nonenzymatically to the respective phosphine oxide.[7,19,20] Thus, an analogous "activation" by glutathione and subsequent oxidation of the phosphine moiety might in turn lead to the reduction of DTNB, resulting in the observed "overshot" of TNB. In fact the formation of several intermediates related to a breakage of the DTNB disulfide bond (as well as coordinative bonds) could be observed in experiments on triphenylphosphine gold(I) chloride (TPPAuCl) using ^{31}P NMR and MS/MS spectroscopy (see Supporting Information, Figures S2 and S3, Scheme S1).

Inhibition of the Disulfide Reductases TrxR and GR

The inhibition of the activity of the target enzyme TrxR and the structurally closely related GR by the NHC gold complexes **1a**−**4a**, the benzimidazolium salt **2** (as negative control) as well as the gold(I) phosphine species auranofin, triethylphosphine gold(I) chloride (TEPAuCl), and TPPAuCl (as positive controls) was performed using the isolated enzymes.[11] Whereas the non-gold-containing compound **2** was devoid of any activity against both enzymes strong inhibitory effects against TrxR (EC_{50} values between 0.009 and 4.0 μM) and more moderate effects against GR (4.2 to 94 μM) could be noted for all gold(I) complexes (see Table 1). Overall, these results clearly demonstrate that the gold(I) center is necessary for the inhibition of the enzymes and support the assumption of the preferential binding to the selenocysteine residue present in the active site of TrxR. One striking feature observed in these enzymatic studies is that the strong selectivity for TrxR inhibition over GR inhibition, which had been previously described for various gold phosphine derivatives,[15,16] was also found for the here reported series of gold(I) NHC complexes (at least 20-fold lower values for TrxR inhibition compared to GR inhibition).

Table 1. Inhibition of TrxR and GR; Results Are Expressed As Means (± Error) of at Least Two Independent Experiments

	EC_{50} TrxR (μM)	EC_{50} GR (μM)	selectivity (*x*-fold)
auranofin	0.009 (± 0.000)	15 (± 0.1)	1666
TEPG	0.037 (± 0.005)	7.9 (± 0.4)	213
TPPG	0.256 (± 0.002)	4.2 (± 0.7)	16
2	> 50 μM	> 50 μM	
1a	0.399 (± 0.040)	30 (± 2.5)	75
2a	0.361 (± 0.040)	8.7 (± 0.0)	24
3a	0.465 (± 0.006)	9.3 (± 1.7)	20
4a	4.0 (± 1.0)	94 (± 15)	23

With the exception of the diphenylmethylene derivate **4a**, which exhibited a comparably low solubility in the used assay buffer that might explain its significantly lower activity, the gold(I) NHC derivatives displayed strong EC_{50} values against TrxR well below 0.5 μM. Higher activity, however, was noted for the investigated gold(I) phosphine derivatives, which also represent a kinetically more reactive class of gold(I) complexes (as studied in more detail above).

Effects on Cell Proliferation, Apoptosis, ROS Formation, Cell Metabolism and Mitochondrial Respiration

The triggering of antiproliferative effects by the target coordination compounds was investigated in various tumor cell lines (namely, MCF-7 human breast adenocarcinoma, HT-29 and HCT-116 colon carcinoma, and HEP-G2 hepatocellular carcinoma). Relevant activities could be noted for all the complexes in these cell lines. The observed IC_{50} values (in the range of 4.6−14.9 μM with the exception of lower activity of **4a** in HCT-116 and HEP-G2 cells) were generally within the same order of magnitude as noted for gold(I) phosphine species (IC_{50} values in the range of 1−5 μM in the used assay[11,23,24]). These results are in good agreement with other reports on bioactive gold carbene species, which reached activities in the low micromolar range.[25,45] The inactivity (IC_{50} values > 100 μM) of the free benzimidazolium salt **2** confirmed that the gold center was necessary to obtain bioactive species. Interestingly, the tumor selective behavior of other gold(I) NHC complexes[25] could not be confirmed for **1a**−**4a** as comparative experiments in nontumorigenic cell lines (HEK-293 human embryonic kidney cells and HFF human foreskin fibroblasts) afforded similar activities (IC_{50} values in the range of 7.6−32 μM, see Supporting Information, Table S1).

To evaluate the biological potential of benzimidazol-2-ylidene gold(I) complexes in more detail, we investigated **2a** exemplarily for more specific chemotherapeutic properties in various cancer and leukemia cell lines. Video phase contrast microscopic imaging of HT-29 cells exposed to 7.0 μM of **2a**

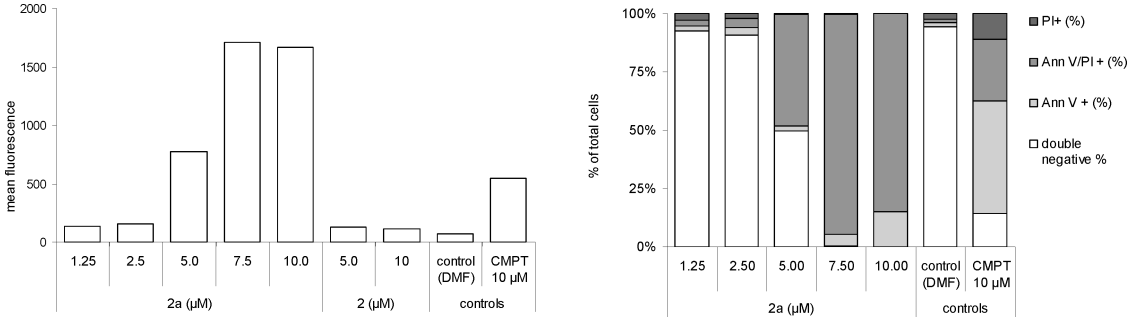

Figure 5. Left: induction of ROS formation by **2** and **2a** in Jurkat cells after 48 h exposure. Similar results were observed after 24 h exposure (see Supporting Information, Figure S5); right: annexin/PI assay for Jurkat cells exposed to **2a** for 48 h. In the Annexin/PI assay, vital cells (double negative) can be distinguished from early apoptotic (AnnV+), late apoptotic (AnnV/PI+), and necrotic (PI+) cells.[48] CMPT served as a positive control.

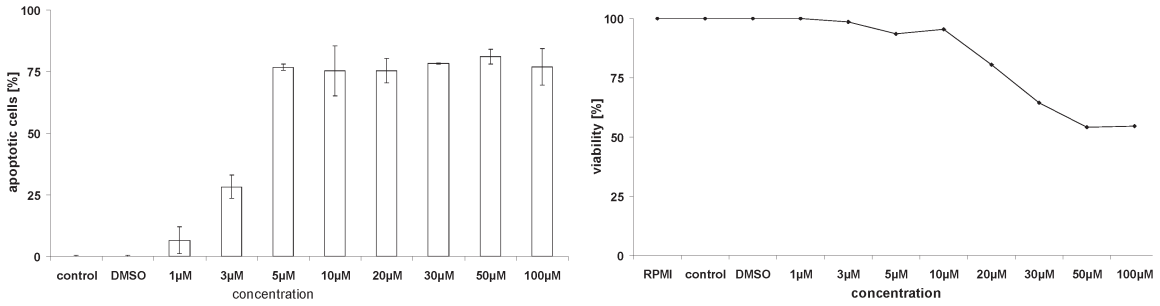

Figure 6. Influence of **2a** on DNA fragmentation (72 h exposure, left) and viability (2 h exposure, LDH release assay, right) in BJAB cells. **2** showed no relevant effects in both assays (see Supporting Information, Figure S7 and Figure S8). Values are given in % of control ± SD (n = 3).

Table 2. IC_{50} Values for Antiproliferative Effects in MCF-7, HT-29, HCT-116, and HEP-G2 Cells, Results Are Expressed As Means (± Error) of at Least Two Independent Experiments

	IC_{50} MCF-7 (μM)	IC_{50} HT-29 (μM)	IC_{50} HCT-116 (μM)	IC_{50} HEP-G2 (μM)
2	> 100	> 100	> 100	> 100
1a	7.5 (± 0.6)	13.3 (± 4.4)	6.7 (± 0.6)	4.9 (± 0.8)
2a	4.6 (± 0.0)	6.4 (± 2.0)	8.4 (± 2.2)	11.2 (± 1.6)
3a	10.2 (± 0.1)	11.8 (± 1.9)	10.0 (± 0.4)	14.9 (± 3.9)
4a	10.3 (± 0.7)	12.3 (± 3.3)	24.6 (± 2.8)	60.7 (± 10.6)

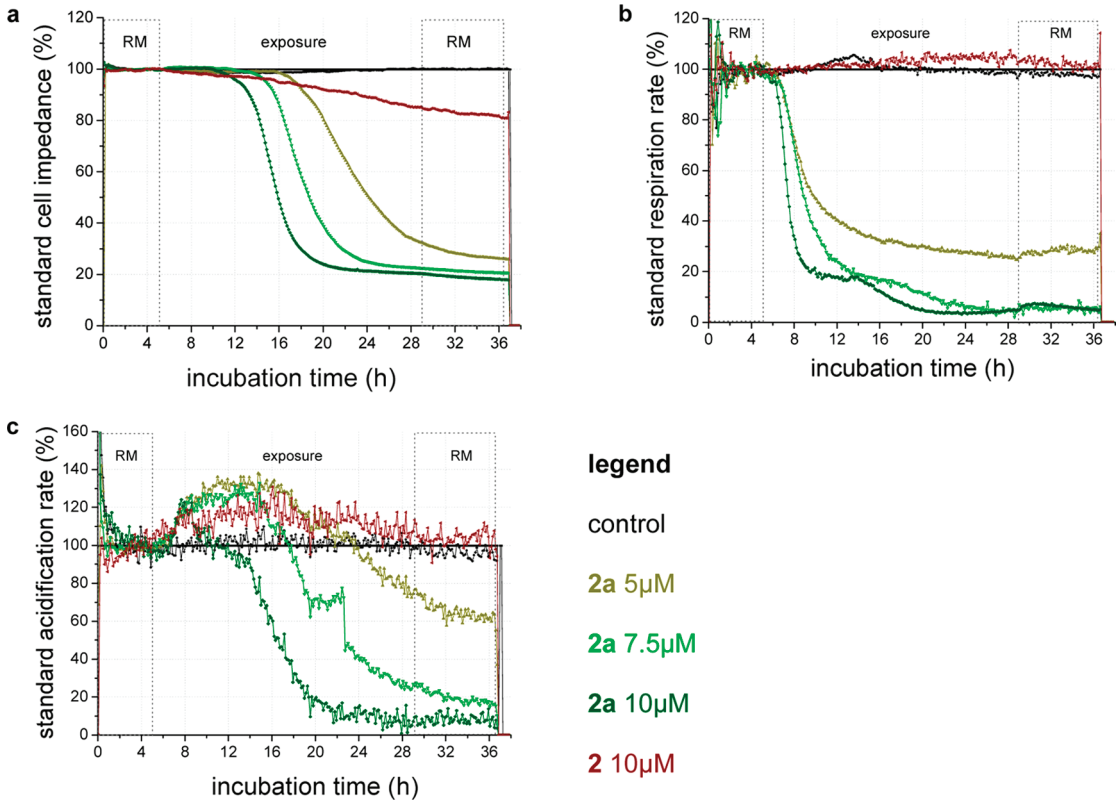

Figure 7. Influence of **2** and **2a** on cell impedance (a), cell respiration (b) and acidification rate (c) in MCF-7 cells; RM, "running medium" (without compound).

for 14 h (Figure S4 and the video files in the Supporting Information) showed the rounding, detachment, and "dying" of single cells, but the cell biomass was overall not strongly reduced during this period. Comparable effects were also observed in an untreated control culture. Therefore, it can be concluded that the above-described effects on cultured tumor cells are rather related to a proliferation inhibition than to a direct cytotoxic effect on the adherent cell monolayer.

Reactive oxygene species (ROS) are products of the physiological mitochondrial cell metabolism and are involved in cellular redox homeostasis. Their induction indicates a perturbation of the cellular antioxidant defense system. In good agreement with the results of the proliferation assay, concentrations higher than 2.5 μM of **2a** strongly induced cellular ROS levels (see Figure 5 left). In contrast, **2** did not trigger ROS production. This pattern correlates also well with the above notion that **2a** selectively affected the activity of the redox relevant enzyme TrxR, whereas **2** had no effect on enzymatic activities. The ability to inhibit the activities of disulfide reductases also under cell culture conditions was confirmed for **2a** and afforded an EC_{50} value of 19.1 μM (see Supporting Information, Figure S6).

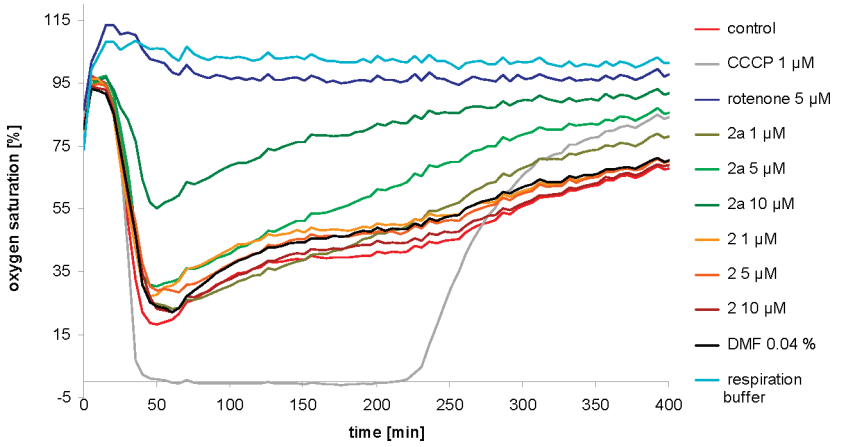

Figure 8. Respiration of freshly isolated mouse liver mitochondria. Mitochondrial activity leads to a decrease in oxygen saturation, which decreases over time (control). Inhibition of mitochondrial activity blocks oxygen consumption, resulting in continuous high oxygen concentration (rotenone, an inhibitor of respiratory chain complex I); decoupling of respiration by carbonyl cyanide 3-chlorophenylhydrazone (CCCP) leads to increased oxygen consumption. The gold complex **2a** leads to a concentration-dependent inhibition of mitochondrial respiration while treatment with **2** shows no effect compared to the untreated control; controls: "blank", buffer without test compound; "DMF", buffer containing the organic solvent but no compound; "respiration buffer", experiment without mitochondria.

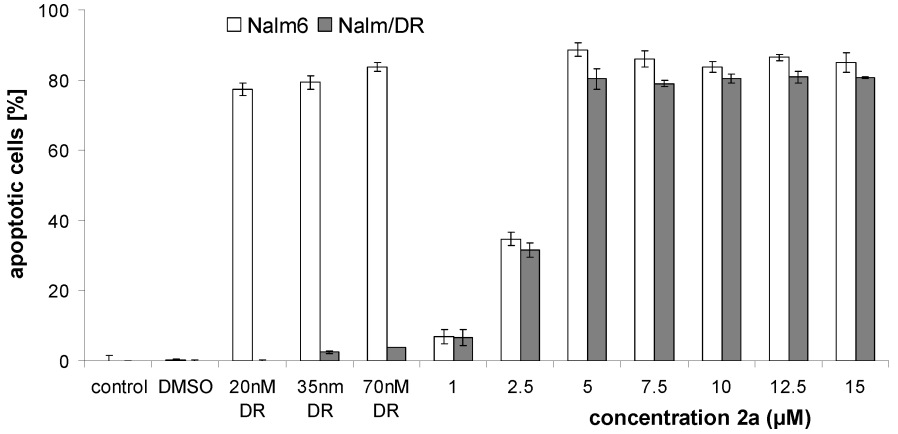

Figure 9. Wildtype and daunorubicine resistant (Nalm/DR) Nalm-6 cells were treated with different concentrations of **2a** and daunorubicine (DR) for 72 h and DNA fragmentation was measured. Relevant doses of DR did not cause a significant DNA fragmentation in Nalm/DR cells. For the treatment with **2a**, both Nalm-6 and Nalm/DR were affected (IC_{50} values: 2.9 μM in Nalm-6 and 3.1 μM in Nalm/DR). Cells treated with blank or DMSO containing cell culture media served as controls. Values are given as percentages of cells with hypodiploid DNA $\pm$ sd ($n = 3$).

Experiments on the apoptosis/necrosis inducing activity of **2a** by the Annexin/propidium iodide (PI) assay showed a strong reduction of vital cells accompanied by a significant relative increase of apoptotic cells in concentrations of 2.5 μM and higher (see Figure 5 right). Additionally, DNA fragmentation, another marker for apoptosis, was strongly increased after exposure to **2a** but not after incubation with **2** (see Figure 6 left).

Short exposure (2 h) lactate dehydrogenase (LDH) release experiments (see Figure 6, right) at higher concentrations (> 10 μM) of **2a** showed a relevant loss of cell vitality, which indicated that first effects took place within a rather short time frame. In overall correlation with its inactivity in the proliferation experiments (see Table 2), **2** did not influence cell viability in this assay up to the highest concentration investigated (100 μM).

Next the influence of **2** and **2a** on cellular metabolism was monitored online by use of a metabolic sensor chip analysis system, which allows the evaluation of the impedance of the cell layer and the respiration rate (oxygen consumption) as well as the acidification rate (glycolysis) of living cells over an extended time span (see Figure 7).[46,47] The impedance of the cells started to decrease in a concentration dependent manner after an exposure of approximately 7 h to **2a**. This indicated morphological changes of the cells, changes in cell membranes, cell−cell contacts, and cellular adhesion, reflecting the induction and onset of cell death (see Figure 7a). Immediate effects of the gold species were reduced oxygen consumption and an increased glycolysis starting at the same time. The latter only increased initially, suggesting a compensatory enhanced glycolysis to compensate for the reduced respiration (see Figure 7b,c). After longer exposure also the acidification rate decreased in a concentration dependent manner, which can be ascribed to the "dying" of the cells. Interestingly, there was no recovery of cellular metabolism when **2a** was withdrawn after 24 h, which indicates that the effects were irreversible. Compound **2** triggered only minor effects at higher concentration on cell impedance but was inactive otherwise. This again demonstrates the importance of the gold(I) central atom.

As the inhibition of TrxR should lead to antimitochondrial effects, which have also been reported for an increasing number of gold metallodrugs,[25,29] we evaluated the effects of **2** and **2a** on mitochondrial respiration of isolated mice liver mitochondria (see Figure 8). In this assay, the oxygen saturation

of a buffer medium is lowered by respirating (functionally active) mitochondria. Impairment of mitochondrial vital functions will antagonize this effect. As expected, exposure to **2a** led to a concentration dependent decrease of mitochondrial respiration while **2** remained again without effect.

Effects on Drug Resistant Cell Lines

Drug resistance phenomena have a major impact on current therapy regimens and cause frequent treatment failures. The major reasons are found with alterations in drug transport processes or the up/down regulation of relevant metabolizing enzymes or molecular targets, thus causing a complex multifactorial event. Novel compounds with different chemical structures and biological properties in some cases can address these highly relevant issues.

Here we studied the effects of **2a** on the apoptosis induction in wild type and doxorubicin, daunorubicin, and vincristin resistant BJAB and Nalm-6 leukemia cells. Western blot studies confirmed the overexpression of P-glycoprotein in the resistant cells (see Supporting Information, Figure S9). The most marked effects of **2a** were observed in daunorubicin resistant Nalm-6 cells, where **2a** caused in the whole investigated concentration range (1.0−15.0 μM) the same extent of DNA fragmentation as in the respective wild type cells (see Figure 9). In vincristine resistant Nalm-6 cells, similar effects were observed at concentrations above 7.5 μM of **2a** (see Supporting Information, Figure S10). In the resistant types of BJAB cells, however, the resistance effects could only be partially reversed (see Supporting Information, Figures S11 and S12).

Conclusions

A series of benzimidazol-2-ylidene gold(I) complexes was prepared, structurally characterized, and biologically investigated. Stability studies against inactivation by the tripeptide glutathione showed that the here presented gold(I) NHC complexes **1a**−**4a** remained rather unaffected. The comparable strong "thiol-based" metabolism of gold(I) phosphines such as auranofin has so far hampered the development of novel drug candidates out of this class.[19,20,49] Accordingly, the choice of NHC ligands probably provides an useful strategy for gold(I) drug design in terms of an enhanced biological stability and also more predictable drug−target interactions.

Studies on the inhibition of disulfide reductases (see Table 2) pointed overall to a strong and selective inhibition of the selenocysteine containing TrxR and confirmed this enzyme as one of the major targets for the here studied gold(I) complexes. The interaction with GR (and the putative Cys284 binding site) supposedly play a role only at higher exposure concentrations. This pattern is also in good agreement with the low reactivity against the thiol of reduced glutathione. Concerning the enzymatic inhibition studies, this is to the best of our knowledge the first report providing EC_{50} values for the direct and selective TrxR inhibition by gold(I) NHC complexes while the inhibition of TrxR in cellular lysates has already been reported previously.[25] However, the expected increase in activity with increasing the lipophilicity/surface volume of the residues at the benzimidazol-2-ylidene nitrogens could not be observed (compare results for **1a**−**4a** in Table 2). Antiproliferative effects for **1a**−**4a** were noted in the low micromolar range, and more detailed experiments on **2a** showed that these effects could be related to the induction of ROS formation, finally resulting in apoptosis and necrosis of the cells as well as to direct effects on mitochondrial integrity (as evidenced by a decrease of mitochondrial respiration). Cellular metabolism studies on the influence on cell impedance, respiration, and acidification rate indicated that the described effects on cell physiology were induced within a rather short time frame of a few hours and were generally irreversible. In analogy, LDH release studies showed that cell viability could be affected after short exposure to **2a** at higher concentrations. It should also be noted that the free ligand **2** was ineffective in all comparative experiments, which confirmed that the presence of the gold(I) center was necessary to obtain compounds with the described bioactivities. Experiments in P-glycoprotein overexpressing daunorubicine, vincristine, and doxorubicine resistant cell lines indicated that the here investigated type of bioorganometallics might find also application in the treatment of certain drug resistant malignancies.

Overall, the here observed overall pharmacodynamic pattern of gold(I) NHC species exhibits several important key features of state-of-the-art novel anticancer drugs, suggesting further development of the here studied class of gold(I) NHC complexes.

Experimental Section

General. All reagents and the solvents were used as received from Sigma, Aldrich, or Fluka. ^{1}H NMR and ^{13}C NMR were recorded on a Bruker DRX-400 AS NMR System, MS spectra were recorded on a Finnigan MAT 4515. The purity of the target compounds (>95%) was confirmed by elemental analysis (Flash EA112, Thermo Quest Italia). For all compounds undergoing biological evaluation, the experimental values differed less than 0.5% from the calculated ones.

Molecular Modeling. As a starting point for rational design, we used the X-ray structure of GR complexed with the GOPI residue 2-(2-phenyl-3-pyridin-2-yl-4,5,6,7-tetrahydro-2*H*-isophosphoindol-1-yl)pyridine (PDB entry 1AAQ) and derived a 3D pharmacophore using the software LigandScout 3.0 as shown in Figure 2.[17,50,51] LigandScout identified lipophilic contacts to Leu261, Leu183, and Ile175, which served as a basis for assumptions leading to the new compounds presented in this work. The 3D overlay of TrxR (2CFY) and GR (2AAQ) was performed using the molecular modeling package MOE (Molecular Operating Environment, version 2009.10, Chemical Computing Group, Montreal, Canada) and is based on a sequence alignment of the two proteins with a subsequent 3D overlay. The alignment confirmed the close relationship between TrxR and GR described by Sandalova et al. previously.[52]

Synthesis. General Procedure for Synthesis of the Benzimidazolium Halide Salts. Benzimidazole (0.118 g, 1.0 mmol), the respective alkyl halogenide (3.0 mmol) and K_2CO_3 (0.138 g, 1.0 mmol) were heated under reflux conditions in acetonitrile for 8 h. The solvent of the resulting suspension was removed under reduced pressure, and the residue was resuspended in dichloromethane and filtered to remove the formed potassium halogenide. The filtrate was evaporated under reduced pressure, the residue was resuspended in tetrahydrofuran and filtered to give the pure product.

1,3-Dimethylbenzimidazoliumiodide (1).[53] Yield: 0.238 g (0.8 mmol, 87%) white powder; mp 217 °C. ^{1}H NMR (DMSO-d_6): (ppm) 4.08 (s, 6H, CH_3), 7.71 (dd, 2H, J = 3.2 Hz, J = 6.3 Hz, $ArH_{4/7}$), 8.02 (ddd, 2H, J = 3.2 Hz, J = 6.3 Hz, $ArH_{5/6}$), 9.64 (s, 1H, NHC). Elemental analysis for $C_9H_{11}N_2I$ (% calcd/found): C (39.44/39.04), H (4.05/4.54), N (10.22/10.00).

1,3-Diethylbenzimidazoliumiodide (2).[53] Yield: 0.272 g (0.9 mmol, 90%) white powder; mp 240 °C. ^{1}H NMR (DMSO-d_6): (ppm) 1.55 (t, 6H, J = 9.7 Hz, CH_3), 4.52 (q, 4H, J = 9.7 Hz, CH_2), 7.68 (dd, 2H, J = 4.2 Hz, J = 8.4 Hz, ArH_4), 8.10 (dd, 2H, J = 4.2 Hz, J = 8.4 Hz, ArH_5), 9.8 (s, 1H, NHC). ^{13}C NMR (DMSO-d_6): (ppm) 14.1 (CH_3) 42.0 (CH_2) 113 (ArC_8) 126

(ArC_4) 130 (ArC_5) 141 (NHC). Elemental analysis for $C_{11}H_{15}N_2I$ (% calcd/found): C (43.73/43.80), H (5.00/5.02), N (9.27/9.13).

1,3-Dibenzylbenzimidazoliumbromide (3).[54] Yield: 0.323 g (0.8 mmol, 76%) white powder; mp 150 °C. ^{1}H NMR (DMSO-d_6): (ppm) 5.81 (s, 4H, CH_2), 7.46 (m, 10H, ArH), 7.64 (dd, 2H, J = 3.1 Hz, J = 6.3 Hz, $ArH_{4/7}$), 7.98 (ddd, 2H, J = 3.2 Hz, J = 6.3 Hz, $ArH_{5/6}$), 10.12 (s, 1H, NHC). Elemental analysis for $C_{21}H_{19}N_2Br$ (% calcd/found): C (66.30/65.41), H (5.26/5.20), N (7.36/6.79).

1,3-Bis-(diphenylmethyl)benzimidazoliumchloride (4).[55] Yield: 0.462 g (0.8 mmol, 80%) white powder; mp 254 °C. ^{1}H NMR ($CDCl_3$): (ppm) 7.45 (m, 24H, ArH), 7.82 (s, 2H, CH), 10.68 (s, 1H, NHC). Elemental analysis for $C_{33}H_{27}N_2Cl$ (% calcd/found): C (81.48/80.99), H (5.55/5.54), N (5.76/5.60).

General Procedure for Synthesis of the Gold NHC Complexes. The respective benzimidazolium salt (1.0 mmol) was treated with Ag_2O (0.116 g, 0.5 mmol) under vigorous stirring in dichloromethane for 5 h. After the color change, dimethylsulfidegold(I) (0.296 g, 1.0 mmol) was added and the reaction was stirred for another 10 h. The obtained suspension was filtered over Celite (281 nm), and the solvent was evaporated under reduced pressure to give the pure product.

Chloro-(1,3-dimethylbenzimidazol-2-ylidene)gold(I) (1a).[53] Yield: 0.095 g (0.3 mmol, 25%) yellow powder. ^{1}H NMR ($CDCl_3$): (ppm) 3.99 (s, 6H, CH_3), 7.46 (m, 4H, ArH). MS(EI): 378 ($M + H^+$). Elemental analysis for $C_9H_{10}AuClN_2$ (% calcd/found): C (28.55/28.56), H (2.60/2.69), N (7.40/6.98).

Chloro-(1,3-diethylbenzimidazol-2-ylidene)gold(I) (2a).[53] Yield: 0.122 g (0.3 mmol, 30%) pale-yellow powder. ^{1}H NMR ($CDCl_3$): (ppm) 1.55 (t, 6H, J = 5.9 Hz, CH_3), 4.54 (q, 4H, J = 9.8 Hz, CH_2), 7.46 (m, 4H, ArH). ^{13}C NMR ($CDCl_3$): (ppm) 15.4 (CH_3), 43.9 (CH_2), 111 (ArC_8), 124 (ArC_4), 132 (ArC_5), 177 (NHC). MS(EI) 406 ($M + H^+$). Elemental analysis for $C_{11}H_{14}AuClN_2$ (% calcd/found): C (32.49/32.03), H (3.47/3.38), N (6.89/6.91).

Chloro-(1,3-dibenzylbenzimidazol-2-ylidene)gold(I) (3a). Yield: 0.265 g (0.5 mmol, 50%) white powder. ^{1}H NMR ($CDCl_3$): (ppm) 5.76 (s, 4H, CH_2), 7.35 (m, 14H, ArH). MS(EI): 530 ($M - H^+$). Elemental analysis for $C_{21}H_{18}AuClN_2$ (% calcd/found): C (47.52/47.72), H (3.42/3.58), N (5.28/5.25).

Chloro-[1,3-bis-(diphenylmethyl)benzimidazol-2-ylidene]gold-(I) (4a). Yield: 0.375 g (0.6 mmol, 55%) white powder. ^{1}H NMR ($CDCl_3$): (ppm) 7.05 (dd, 2H, J = 3.5 Hz, J = 6.5 Hz, $ArH_{4/7}$), 7.36 (m, 22H, ArH), 7.89 (s, 2H, CH). MS (EI) 682 ($M + H^+$). Elemental analysis for $C_{33}H_{26}AuClN_2$ (% calcd/found): C (58.03/57.75), H (3.84/3.87), N (4.10/3.87).

Reaction with Glutathione. The gold(I) complexes were prepared as stock solutions in dimethylformamide (DMF) and diluted with potassium phosphate buffer pH 7.0 to achieve a final concentration of 500 μM (DMF: 0.2% V/V). To 25 μL of 250 μM aqueous solutions of reduced glutathione, each 25 μL of the respective potassium phosphate buffer solution (containing the compounds or only the DMF vehicle as control) and 25 μL 100 mM aqueous EDTA solution pH 7.5 were added and the resulting solutions were incubated with moderate shaking in a 96-well plate at 37 °C for 20 or 60 min. To each well, 200 μL of reaction mixture (1000 μL reaction mixture consisted of 620 μL potassium phosphate buffer pH 7.0, 80 μL 100 mM EDTA solution pH 7.5, and 300 μL distilled water) were added, and the reaction was started with the addition of 25 μL of a 20 mM ethanolic solution of DTNB. After proper mixing, the formation of 5-TNB was monitored in a microplate reader (Perkin-Elmer Victor X4) at 405 nm. For each tested compound, the noninterference with the assay components was confirmed by a negative control experiment using a glutathione free solution. Results are presented as means of two independent experiments.

TrxR and GR Inhibition Assay. To determine the inhibition of TrxR and GR an established microplate reader based assay was performed with minor modifications.[11,56] For this purpose, commercially available rat liver TrxR and baker's yeast GR (both from Sigma-Aldrich) were used and diluted with distilled water to achieve a concentration of 2.0 U/mL. The compounds were freshly dissolved as stock solutions in DMF. To each, 25 μL aliquots of the enzyme solution each 25 μL of potassium phosphate buffer pH 7.0 containing the compounds in graded concentrations or vehicle (DMF) without compounds (control probe) were added and the resulting solutions (final concentration of DMF: 0.5% V/V) were incubated with moderate shaking for 75 min at 37 °C in a 96-well plate. To each well, 225 μL of reaction mixture (1000 μL reaction mixture consisted of 500 μL potassium phosphate buffer pH 7.0, 80 μL 100 mM EDTA solution pH 7.5, 20 μL BSA solution 0.05%, 100 μL of 20 mM NADPH solution, and 300 μL of distilled water) were added and the reaction started by addition of 25 μL of an 20 mM ethanolic DTNB solution. After proper mixing, the formation of 5-TNB was monitored with a microplate reader (Perkin-Elmer Victor X4) at 405 nm in 10 s intervals for 6 min. The increase in 5-TNB concentration over time followed a linear trend ($r^2 \geq 0.99$), and the enzymatic activities were calculated as the slopes (increase in absorbance per second) thereof. For each tested compound, the noninterference with the assay components was confirmed by a negative control experiment using an enzyme-free solution. The EC_{50} values were calculated as the concentration of compound decreasing the enzymatic activity of the untreated control by 50% and are given as the means and error of repeated experiments.

Cell Culture. MCF-7 breast adenocarcinoma, HT-29 and HCT-116 colon carcinoma, and HEP-G2 hepatocellular carcinoma cells were maintained in DMEM high glucose (PAA) supplemented with 50 mg/L gentamycin and 10% (V/V) fetal calf serum (FCS) prior to use. Leukemia B-cell precursor (Nalm-6) and its Vincristin and Daunorubicin resistant sublines, Burkitt-like lymphoma cells (BJAB) and its Doxorubicin resistant (7CCA) and Vincristin resistant (BIBO) sublines, were cultured in RPMI 1640 supplemented with 10% FCS.

Antiproliferative Effects in MCF-7, HT-29, HCT-116, and HEP-G2 Cells. The antiproliferative effects in MCF-7, HT-29, HCT-116, and HEP-G2 cells after 72 h (HT-29, HCT-116) or 96 h (MCF-7, HEP-G2) exposure to the gold complexes were evaluated according to an established procedure.[23] For the experiments, the compounds were prepared freshly as stock solutions in DMF and diluted with the cell culture medium to the final assay concentrations (0.1% V/V DMF). The IC_{50} value was described as that concentration reducing proliferation of untreated control cells by 50%.

ROS Formation. Jurkat cells were cultivated under standard conditions and cells were incubated with the compounds for 24 h as indicated. After incubation, cells were collected, centrifuged at 0.2g (1500 rpm), and resuspended in FACS buffer (D-PBS, Gibco, + 1% BSA, PAA). Cell suspensions were treated with DHE (dihydroethidium, SIGMA, 5 μL of 5 mM stock solution per 1.0 mL of cell suspension containing 10^6 cells) at room temperature in the dark for 15 min, washed one more time with FACS buffer, and immediately analyzed using a FACSCalibur (Becton Dickinson) and CellQuest Pro (BD) analysis software. Excitation and emission settings were 488 nm and 564−606 nm (FL2 filter), respectively. Important note: although DHE is known to interact only with superoxide anion, the intensity of fluorescence is commonly considered as a reflection of total intracellular ROS.

Annexin V/PI Staining. Jurkat cells were treated with the indicated concentration of the substance for 48 h, collected, and stained with Annexin V-FITC (eBioscience) according to the manufacturers recommendation. Briefly, approximately 5.0 × 10^5 cells were resuspended in 50 μL of Annexin V staining buffer (10 mM HEPES, 140 mM NaCl, and 2.5 mM $CaCl_2$, pH 7.4), 2.5 μL of Annexin V conjugate, and 1.25 μL of PI solution (1 mg/mL) were added and the probes were incubated in the dark at room temperature for 15 min. Signal intensity was analyzed using a FACSCalibur (Becton Dickinson) and CellQuest Pro (BD) analysis software. Excitation and emission settings were 488 nm,

515−545 nm (FL1 channel) for Annexin V-FITC and 564−606 nm (FL2 channel) for PI.

LDH Release Assay. After incubation with different concentrations of **2** and **2a** for 2 h, LDH released by BJAB cells was measured in cell culture supernatants using a cytotoxicity detection kit from Boehringer Mannheim (Mannheim, Germany). The supernatants were centrifuged at 300*g* for 5 min. Cell-free supernatants (20 μL) were diluted with 80 μL of PBS and 100 μL of reaction mixture were added. Then, the time-dependent formation of the reaction product was quantified photometrically at 490 nm. The maximum amount of LDH activity released by the cells was determined by lysis of the cells using 0.1% Triton X-100 in culture medium and was set as 100% cell death.

Measurement of DNA Fragmentation. Apoptotic cell death was determined by a modified cell cycle analysis, which detects DNA fragmentation at the single cell level. For measurement of DNA fragmentation cells were seeded at a density of 1×10^5 cells/mL and treated with different concentrations of **2** and **2a**. After 72 h of incubation, cells were collected by centrifugation at 30*g* for 5 min, washed with PBS at 4 °C, and fixed in PBS/2% (v/v) formaldehyde on ice for 30 min. After fixation, cells were incubated with ethanol/PBS (2:1, v/v) for 15 min, pelleted, and resuspended in PBS containing 40 μg/mL RNase A. After incubation for 30 min at 37 °C, cells were pelleted again and finally resuspended in PBS containing 50 μg/mL PI. Nuclear DNA fragmentation was then quantified by flow cytometric determination of hypodiploid DNA. Data were collected and analyzed using a FACScan (Becton Dickinson, Heidelberg, Germany) equipped with the CELLQuest software. Data are given in % hypoploidy (subG1), which reflects the number of apoptotic cells.

Effects on Cell Metabolism. Online measurement of cell metabolism and morphological changes was done using a Bionas 2500 sensor chip system (Bionas, Rostock, Germany). The metabolic sensor chips (SC 1000) include ion-sensitive field-effect transistors to record pH changes, an oxygen electrode to monitor oxygen consumption, and interdigitated electrode structures to measure impedance under the cell layer. Approximately 1.5×10^5 cells were seeded directly onto each sensor chip in 450 μL of DMEM (PAA, E15−883) with penicillin/streptomycin and 10% (v/v) FCS (PAA) and incubated at 37 °C, 5% CO_2, and 95% humidity for 24 h. The cell number used resulted in approximately 80−90% confluence of the cells on the chip surface after 24 h. This was the starting condition for online monitoring. Sensor chips with cells were then transferred to the Bionas2500 analyzer in which medium is continuously exchanged in 8 min cycles (4 min exchange of medium and 4 min without flow), during which the parameters were measured. The running medium used during analysis was DMEM without carbonate buffer and only weakly buffered with 1 mM Hepes and reduced FCS (0.1%). For drug activity testing, the following steps were included: (1) 5 h equilibration with running medium (RM), (2) drug incubation with substances freshly dissolved in medium at indicated concentrations and indicated incubation time, (3) a regeneration step in which cells are again fed with running medium without substances, and (4) at the end of each experiment, the cell membrane was damaged by addition of 0.2% Triton X-100 to obtain a basic signal without living cells on the sensor surface as a negative control.

Isolation of Mouse Liver Mitochondria. Mitochondria were isolated according to described procedures with minor modifications.[57,58] Mouse (wildtype, C57BL/6) liver mitochondria were isolated by Dounce homogenization and differential centrifugation. The entire isolation took place in isolation buffer (300 mM trehalose, 10 mM HEPES-KOH pH 7,7, 10 mM KCl, 1 mM EGTA, 1 mM EDTA, 0.1% fatty acid free BSA). The homogenate was centrifuged for 5 min at 1000 g and 4 °C. The supernatant was collected and centrifuged for 2 min at 15800 g and 4 °C. The mitochondrial pellet was resuspended in a small volume of isolation buffer, and the last centrifugation step was repeated. After resuspending the final mitochondria pellet in isolation buffer, the protein content was estimated by the Bradford Assay.

Measurement of Mitochondrial Oxygen Consumption. The measurement was performed using OxoPlate (PreSens, Germany) 96-well plates which contain an immobilized oxygen sensor at the bottom of each well. Fluorescence is measured in dual mode (excitation 540 nm and emission 650 nm) with reference emission 590 nm. The signal ratio 650/590 nm corresponds to the oxygen partial pressure. The calibration of the fluorescence reader is performed using a two-point calibration with oxygen-free water (1% Na_2SO_3) and air-saturated water with oxygen partial pressure corresponding to 0% and 100% respectively. Then 18 μg of freshly isolated mitochondria were suspended in 100 μL of respiration buffer (25 mM sucrose, 100 mM KCl, 75 mM mannitol, 5 mM $MgCl_2$, 10 mM KH_2PO_4, 0.5 mM EDTA, 10 mM TRIS, 0.1% fatty acid-free BSA, pH 7.4) containing 10 mM pyruvate, 2 mM malate, 2 mM ADP, and 0.5 mM ATP to activate oxidative phosphorylation. The mitochondrial suspensions also contained the test compounds in the indicated concentrations. Fluorescence was measured continuously for 400 min with kinetic intervals of 5 min by a Tecan Safire^2 (Tecan, Maennedorf, Switzerland) microplate reader at 37 °C. During the measurements, the plates were sealed with a breathable membrane (Diversified Biotech, Boston, MA). Additional controls were 5 μM rotenone (Sigma-Aldrich) as inhibitor of respiratory chain complex I and 1 μM CCCP (carbonyl cyanide 3-chlorophenylhydrazone, Sigma-Aldrich) as uncoupling agent, capable of increasing electron flow through the respiratory chain thereby increasing the oxygen consumption.

Acknowledgment. Financial support by Deutsche Forschungsgemeinschaft (DFG, grant FOR-630) is gratefully acknowledged.

Supporting Information Available: More details on the reaction of a gold(I) phosphine complex with glutathione (^{31}P NMR and ESI-MS experiments), additional data on the effects on cell proliferation of non tumorigenic cells, video microscopic imaging, ROS formation, inhibition of disulfide reductases in cells, DNA fragmentation, cell viability, and effects in resistant cell lines are presented as a PDF file and as two video files. This material is available free of charge via the Internet at http://pubs.acs.org.

References

(1) Ott, I.; Gust, R. Non-platinum Metal Complexes as Anti-cancer Drugs. *Arch. Pharm. Chem. Life Sci.* **2007**, *340*, 117–126.
(2) vanRijt, S. H.; Sadler, P. Current applications and future potential for bioinorganic chemistry in the development of anticancer drugs. *Drug Discovery Today* **2009**, *14*, 1089–1097.
(3) Gasser, G.; Ott, I.; Metzler-Nolte, N. Organometallic Anticancer Compounds. *J. Med. Chem.* **2010**, *53*, doi: 10.1021/jm100020w.
(4) Tiekink, E. R. T. Gold derivatives for the treatment of cancer. *Crit. Rev. Oncol. Hematol.* **2002**, *42*, 225–248.
(5) Ott, I. On the medicinal chemistry of gold complexes as anticancer drugs. *Coord. Chem. Rev.* **2009**, *253*, 1670–1681.
(6) Bindoli, A.; Rigobello, M. P.; Scutari, G.; Gabbiani, C.; Casini, A.; Messori, L. Thioredoxin reductase: a target for gold compounds acting as potential anticancer drugs. *Coord. Chem. Rev.* **2009**, *253*, 1692–1707.
(7) Nobili, S.; Mini, E.; Landini, I.; Gabbiani, C.; Casini, A.; Messori, L. Gold Compounds as Anticancer Agents: Chemistry, Cellular Pharmacology, and Preclinical Studies. *Med. Res. Rev.* **2010**, *30*, 550–580.
(8) Gandin, V.; Fernandes, A. P.; Rigobello, M. P.; Dani, B.; Sorrentino, F.; Tisato, F.; Björnstedt, M.; Bindoli, A.; Sturaro, A.; Rella, R.; Marzano, C. Cancer Cell Death Induced by Phosphine Gold(I) Compounds Targeting Thioredoxin Reductase. *Biochem. Pharmacol.* **2010**, *79*, 90–101.
(9) Caruso, F.; Villa, R.; Rossi, M.; Pettinari, C.; Paduano, F.; Pennati, M.; Daidone, M. G.; Zaffaroni, N. Mitochondria are

primary targets in apoptosis induced by the mixed phosphine gold species chlorotriphenylphosphine-1,3-bis(diphenylphosphino)-propanegold(I) in melanoma cell lines. *Biochem. Pharmacol.* **2007**, *73*, 773–781.
(10) Rigobello, M. P.; Folda, A.; Dani, B.; Menabò, R.; Scutari, G.; Bindoli, A. Gold(I) complexes determine apoptosis with limited oxidative stress in Jurkat T cells. *Eur. J. Pharmacol.* **2008**, *582*, 26–34.
(11) Ott, I.; Qian, X.; Xu, Y.; Vlecken, D. H. W.; Marques, I. J.; Kubutat, D.; Will, J.; Sheldrick, W. S.; Jesse, P.; Prokop, A.; Bagowski, C. P. A Gold(I) Phosphine Complex Containing a Naphthalimide Ligand Functions as a TrxR Inhibiting Antiproliferative Agent and Angiogenesis Inhibitor. *J. Med. Chem.* **2009**, *52*, 763–770.
(12) Magherini, F.; Modesti, A.; Bini, L.; Puglia, M.; Landini, I.; Nobili, S.; Mini, E.; Cinellu, M. A.; Gabbiani, C.; Messori, L. Exploring the biochemical mechanisms of cytotoxic gold compounds: a proteomic study. *J. Biol. Inorg. Chem.* **2010**, *15*, 573–582.
(13) Gromer, S.; Urig, S.; Becker, K. The Thioredoxin System from Science to Clinic. *Med. Res. Rev.* **2004**, *24*, 40–89.
(14) Arner, E. S. J. Focus on mammalian thioredoxin reductases—important selenoproteins with versatile functions. *Biochim. Biophys. Act.* **2009**, *1790*, 495–526.
(15) Gromer, S.; Arscott, L. D.; Williams, C. H.; Schirmer, R. H.; Becker, K. Human Placenta Thioredoxin Reductase. *J. Biol. Chem.* **1998**, *273*, 20096–20101.
(16) Vergara, E.; Casini, A.; Sorrentino, F.; Zava, O.; Cerrada, E.; Rigobello, M. P.; Bindoli, A.; Laguna, M.; Dyson, P. J. Anticancer Therapeutics That Target Selenoenzymes: Synthesis, Characterization, in Vitro Cytotoxicity, and Thioredoxin Reductase Inhibition of a Series of Gold(I) Complexes Containing Hydrophilic Phosphine Ligands. *ChemMedChem* **2010**, *5*, 96–102.
(17) Urig, S.; Fritz-Wolf, K.; Reau, R.; Herold-Mende, C.; Toth, K.; Davioud-Charvet, E.; Becker, K. Undressing of Phosphine Gold(I) Complexes as Irreversible Inhibitors of Human Disulfide Reductases. *Angew. Chem., Int. Ed.* **2006**, *45*, 1881–1886.
(18) Pratesi, A.; Gabbiani, C.; Ginanneschi, M.; Messori, L. Reactions of medicinally relevant gold compounds with the C-terminal motif of thioredoxin reductase elucidated by MS analysis. *Chem. Commun.* **2010**, *46*, 7001–7003.
(19) Shaw, C. F. Gold-based therapeutic agents. *Chem. Rev.* **1999**, *99*, 2589–2600.
(20) Coffer, M. T.; Shaw, C. F.; Hormann, A. L.; Mirabelli, C. K.; Crooke, S. T. Thiol Competition for Et_3PAuS-Albumin: A Nonenzymatic Mechanism for Et_3PO Formation. *J. Inorg. Biochem.* **1987**, *30*, 177–187.
(21) Kinsch, E. M.; Stephan, D. W. A ^{31}P nuclear magnetic resonance and fluorescence study of the interaction of an anti-arthritic gold phosphine drug with albumin. A bioinorganic approach. *Inorg. Chim. Act.* **1984**, *91*, 263–267.
(22) Mirabelli, C. K.; Johnson, R. K.; Hill, D. T.; Faucette, L. F.; Girard, G. R.; Kuo, G. Y.; Sung, C. M.; Crooke, S. T. Correlation of the in Vitro Cytotoxic and in Vivo Antitumor Activities of Gold(I) Coordination Complexes. *J. Med. Chem.* **1986**, *29*, 218–223.
(23) Scheffler, H.; You, Y.; Ott, I. Comparative studies on the cytotoxicity, cellular and nuclear uptake of a series of chloro gold(I) phosphine complexes. *Polyhedron* **2010**, *29*, 66–69.
(24) Bagowski, C. P.; You, Y.; Scheffler, H.; Vlecken, D. H.; Schmitz, D. J.; Ott, I. Naphthalimide Gold(I) Phosphine Complexes as Anticancer Metallodrugs. *Dalton Trans.* **2009**, 10799–10805.
(25) Hickey, J. L.; Ruhayel, R. A.; Barnard, P. J.; Baker, M. V.; Berners-Price, S. J.; Filipovska, A. Mitochondria-targeted chemotherapeutics: the rational design of gold(I) *N*-heterocyclic carbene complexes that are selectively toxic to cancer cells and target protein selenols in preference to thiols. *J. Am. Chem. Soc.* **2008**, *130*, 12570–12571.
(26) Deponte, M.; Urig, S.; Arscott, L. D.; Fritz-Wolf, K.; Réau, R.; Herold-Mende, C.; Koncarevic, S.; Meyer, M.; Davoiud-Charvet, E.; Ballou, D. P.; Williams, C. H.; Becker, K. Mechanistic Studies on a Novel, Highly Potent Gold-Phosphole Inhibitor of Human Glutathione Reductase. *J. Biol. Chem.* **2005**, *280*, 20628–20637.
(27) Baker, M.; Barnard, P. J.; Berners-Price, S. J.; Brayshaw, S. K.; Hickey, J. L.; Skelton, B. W.; White, A. H. Cationic, linear Au(I) *N*-heterocyclic carbene complexes: synthesis, structure and anti-mitochondrial activity. *Dalton Trans.* **2006**, 3708–3715.
(28) Jellicoe, M. M.; Nichols, S. J.; Callus, B. A.; Baker, M. V.; Barnard, P. J.; Berners-Price, S. J.; Whelan, J.; Yeoh, G. C.; Filipovska, A. Bioenergetic differences selectively sensitize tumorigenic liver progenitor cells to a new gold(I) compound. *Carcinogenesis* **2008**, *29*, 1124–1133.
(29) Barnard, P. J.; Berners-Price, S. J. Targeting the mitochondrial cell death pathway with gold compounds. *Coord. Chem. Rev.* **2007**, *251*, 1889–1902.
(30) Tonner, R.; Heydenrych, G.; Frenking, G. Bonding Analysis of *N*-Heterocyclic Carbene Tautomers and Phosphine Ligands in Transition-Metal Complexes: A Theorical Study. *Chem.—Asian J.* **2007**, *2*, 1555–1567.
(31) Hahn, F. E. Heterocyclic Carbenes: Synthesis and Coordination Chemistry. *Angew. Chem., Int. Ed.* **2008**, *47*, 3122–3172.
(32) Yan, J. J.; Chow, A. L.-F.; Leung, C.-H.; Sun, R. W.-Y.; Ma, D.-L.; Che, C.-M. Cyclometalated gold(III) complexes with *N*-heterocyclic carbene ligands as topoisomerase I poisons. *Chem. Commun.* **2010**, *46*, 3893.
(33) Cetinkaya, B.; Cetinkaya, E.; Kucubay, H.; Durmaz, R. Antimicrobal activity of carbene complexes of rhodium(I) and ruthenium(II). *Arzneim. Forsch.* **1996**, *46*, 821–823.
(34) Teyssot, M.; Jarrousse, A.; Chevry, A.; Haze, A. D.; Beaudoin, C.; Manin, M.; Nolan, S. P.; Diez-Gonzalez, S.; Morel, L.; Gautier, A. Toxicity of copper(I)−NHC complexes against human tumor cells: induction of cell cycle arrest, apoptosis, and DNA cleavage. *Chem.—Eur. J.* **2009**, 15.
(35) Teyssot, M.-L.; Jarrousse, A.-S.; Manin, M.; Chevry, A.; Roche, S.; Norre, F.; Beaudoin, C.; Morel, L.; Boyer, D.; Mahiou, R.; Gautier, A. Metal−NHC complexes: a survey of anti-cancer properties. *Dalton Trans.* **2009**, 6894–6902.
(36) Skander, M.; Retailleau, P.; Bourrie, B.; Schio, L.; Mailliet, P.; Marinetti, A. *N*-Heterocyclic Carbene−Amine Pt(II) Complexes, a New Chemical Space for the Development of Platinum-Based Anticancer Drugs. *J. Med. Chem.* **2010**, *53*, 2146–2154.
(37) Özdemir, İ.; Temelli, N.; Günal, S.; Demir, S. Gold(I) Complexes of *N*-Heterocyclic Carbene Ligands Containing Benzimidazole: Synthesis and Antimicrobial Activity. *Molecules* **2010**, *15*, 2203–2210.
(38) Durmaz, R.; Kücükbay, H.; Cetinkaya, E.; Cetinkaya, B. Antimicrobial Activity of Rhodium(I) and Ruthenium(II) Carbene Complexes Derived from Benzimidazole Against *Staphylococcus aureus* Isolates. *Turk. J. Med. Sci.* **1997**, *27*, 59–61.
(39) Baker, M.; Barnard, P. J.; Brayshaw, S. K.; Hickey, J. L.; Skelton, B. W.; White, A. H. Synthetic, Structural and Spectroscopic Studies of a (Pseudo)halo(1,3-di-*tert*-butylimidazol-2-ylidene)gold Complexes. *Dalton Trans.* **2005**, *37*, 37–42.
(40) Jothibasu, R.; Huynh, H. V.; Koh, L. L. Au(I) and Au(III) Complexes of a Sterically Bulky Benzimidazole-Derived *N*-Heterocyclic Carbene. *J. Organomet. Chem.* **2008**, *693*, 374–380.
(41) Fremont, P.; Scott, N. M.; Stevens, E. D.; Nolan, S. P. Synthesis and Structural Characterization of *N*-Heterocyclic Carbene Gold-(I) Complexes. *Organometallics* **2005**, *24*, 2411–2418.
(42) Ellman, G. L. A colorimetric method for the determining low concentrations of mercaptams. *Arch. Biochem. Biophys.* **1958**, *74*, 443–450.
(43) Ellman, G. L. Tissue sulfhydryl groups. *Arch. Biochem. Biophys.* **1959**, *82*, 70–77.
(44) Holmgren, A.; Björnstedt, M. Thioredoxin and Thioredoxin Reductase. *Methods Enzymol.* **1995**, *252*, 199–208.
(45) Lemke, J.; Pinto, A.; Niehoff, P.; Vasylyeva, V.; Metzler-Nolte, N. Synthesis, structural characterisation and anti-proliferative activity of NHC gold amino acid and peptide conjugates. *Dalton Trans.* **2009**, 7063–7070.
(46) Ehret, R.; Baumann, W.; Brischwein, M.; Lehmann, M.; Henning, T.; Freund, I.; Drechsler, S.; Friedrich, U.; Hubert, M.-L.; Motrescu, E.; Kob, A.; Palzer, H.; Grothe, H.; Wolf, B. Multiparametric microsensor chips for screening applications. *J. Anal. Chem.* **2001**, *369*, 30–35.
(47) Schatzschneider, U.; Niesel, J.; Ott, I.; Gust, R.; Alborzinia, H.; Wölfl, S. Cellular uptake, cytotoxicity, and metabolic profiling of human cancer cells treated with ruthenium(II) polypyridyl complexes $[Ru(bpy)2(N{-}N)]Cl_2$ with N−N=bpy, phen, dpq, dppz, and dppn. *ChemMedChem* **2008**, *3*, 1104–1109.
(48) Engeland, M. v.; Nieland, L. J. W.; Ramaekers, F. C. S.; Schutte, B.; Reutelingsperger, C. P. M. Annexin V-Affinity Assay: A Review on an Apoptosis Detection System Based on Phosphatidylserine Exposure. *Cytometry* **1998**, *31*, 1–9.
(49) Snyder, R. M.; Mirabelli, C. K.; Crooke, S. T. Cellular association, intracellular distribution, and efflux of auranofin via sequential ligand exchange reactions. *Biochem. Pharmacol.* **1986**, *35*, 923–932.
(50) Wolber, G.; Dornhofer, A. A.; Langer, T. Efficient overlay of small organic molecules using 3D pharmacophores. *J. Comput.-Aided Mol. Des.* **2006**, *20*, 773–788.
(51) Wolber, G.; Langer, T. LigandScout: 3-D pharmacophores derived from protein-bound ligands and their use as virtual screening filters. *J. Chem. Inf. Model.* **2005**, *45*, 160–169.
(52) Sandalova, T.; Zhong, L.; Lindqvist, Y.; Holmgren, A.; Schneider, G. Three-dimensional structure of a mammalian thioredoxin reductase: implications for mechanism and evolution of a selenocysteine-dependent enzyme. *Proc. Natl. Acad. Sci. U.S.A.* **2001**, *98*, 9533–9538.

(53) Wang, H. M. J.; Chen, C. Y. L.; Lin, I. J. B. Synthesis, Structure, and Spectroscopic Properties of Gold(I)−Carbene Complexes. *Organometallics* **1999**, *18*, 1216–1223.
(54) Starikova, O. V.; Dolgushin, G. V.; Larina, L. I.; Ushakov, P. E.; Komarova, T. N.; Lopyrev, V. A. Synthesis of 1,3-Dialkylimidazolium and 1,3-Dialkylbenzimidazolium Salts. *Russ. J. Org. Chem.* **2003**, *39*, 14−67−1470.
(55) Huang, W.; Guo, J.; Xiao, Y.; Zhu, M.; Zou, G.; Tang, J. Palladium−benzimidazolium salt catalyst systems for Suzuki coupling: development of a practical and highly active palladium catalyst system for coupling of aromatic halides with arylboronic acids. *Tetrahedron* **2005**, *61*, 9783–9790.
(56) Smith, A. D.; Morris, V. C.; Levander, O. A. Rapid Determination of Glutathione Peroxidase an Thioredoxin Reductase Activities Using a 96-Well Microplate Format: Comparison to Standard Cuvette-based Assays. *Int. J. Vitam. Nutr. Res.* **2001**, *71*, 87–92.
(57) Yamaguchi, R.; Andreyev, A.; Murphy, A. N.; Perkins, G. A.; Ellisman, M. H.; Newmeyer, D. D. Mitochondria frozen with trehalose retain a number of biological functions and preserve outer membrane integrity. *Cell Death Differ.* **2007**, *14*, 616–624.
(58) Fernández-Vizarra, E.; López-Pérez, M. J.; Enriquez, J. A. Isolation of biogenetically competent mitochondria from mammalian tissues and cultured cells. *Methods* **2002**, *26*, 292–297.